Direct Production of Aluminum Manganese and Silicon Alloys in Aluminum Reduction Cells: A Laboratory Test

Gudrun Saevarsdottir, Omar Awayssa, Rauan Meirbekova, and Geir Martin Haarberg

Abstract

Aluminum smelters produce pure aluminum in reduction cells by the Hall-Héroult process but supply a variety of alloys to their customers. The alloys are produced in the cast house, as master alloys containing the desired alloying elements are added to the primary aluminum from the potroom before casting. In this work, the concept of producing silicon- or manganesecontaining master alloys directly in the aluminum reduction cells, by feeding silicon or manganese oxides into the electrolyte, along with the alumina raw material was investigated. The results in this paper are obtained from a laboratory cell, and the current efficiency for the alloy deposition is estimated.

Keywords

Direct alloy deposition • Aluminum reduction • Aluminum–silicon alloys • Aluminum–manganese alloys • Aluminum • Manganese • Silicon • Aluminum–Manganese Alloys • Aluminum–Silicon alloys • Electrodeposition • Current efficiency

Introduction

Primary aluminum is produced industrially with the Hall-Héroult process by electrolytic reduction of alumina (Al_2O_3), which is dissolved in an electrolyte based on cryolite (Na_3AlF_6) at 960–970 °C. The overall simplified electrochemical reaction is given by [1].

$$2Al_2O_3(\text{dissolved}) + 3C(s) = 4Al(l) + 3CO_2(g) \quad (1)$$

The cathode product of this process is pure molten aluminum, which is transferred to the casthouse where it is solidified. Many casthouses produce specialized products, such as rolling slabs, extrusion bolts, or even specialized alloys for remelting, all based on customer specifications. All these products require alloying elements to be mixed with the primary metal to obtain the desired composition optimized for their specific use. Other treatments, such as refining and specialized casting techniques, are also applied. Alloying is normally done by mixing a master alloy with a high concentration of the desired additive. Manganese is the principal alloying element in the 3xxx aluminum alloys series. A limited percentage of up to 1.5 wt.% Mn added to Al improves corrosion resistance and makes the alloy much stronger than commercial pure aluminum. The improvements in mechanical properties adapt the alloy for the wide use in moderate strength applications requiring good workability [2]. The melting point of manganese is 1245 °C and that of aluminum is 660 °C [3]. The rate of the dissolution of manganese in molten aluminum is very slow which very much depends on the particle size of the added manganese [3]. When manganese in powder form is added to molten aluminum, it may float on the surface and form a hard crust which means some of it may be oxidized. A patent was filed in 1975 by King on a process for the production of aluminum–manganese alloys directly in the cryolite-based melt. According to this invention, aluminum–manganese alloys containing up to 10 wt.% Mn have been prepared by adding either MnO, MnO_2, or their mixtures to aluminum in a cryolite-based electrolyte [4]. This suggests that direct alloy electrodeposition of aluminum–manganese alloys, as reported in this paper, is feasible.

Silicon is the primary alloying element in many important casting alloys of aluminum, as it compensates for the volume

G. Saevarsdottir (✉)
Department of Engineering, Reykjavik University, Menntavegi 1, 102, Reykjavik, Iceland
e-mail: gudrunsa@ru.is

G. Saevarsdottir · O. Awayssa · G. M. Haarberg
Department of Materials Science and Engineering, NTNU, Sem Sælands vei 12, NO-7491 Trondheim, Norway

R. Meirbekova
DTE, Árleynir 8, 108 Reykjavik, Iceland

D. Eskin (ed.), *Light Metals 2022*, The Minerals, Metals & Materials Series,
https://doi.org/10.1007/978-3-030-92529-1_54

contraction of aluminum during solidification [5]. The silicon content may range between 3 and 25%. It is also present in many wrought alloys and is the most important alloying element in the 4xxx series [2, 6]. The addition of aluminum–silicon master alloy in the cast-house comes with its own challenges, so the possibility of direct deposition of aluminum–silicon alloy in the reduction cell is worth pursuing.

Due to the +4 valency of Si in quarts, along with similar molar mass to Al, 29% more energy is required to reduce SiO_2 to Si than Al_2O_3 to Al metal, if the same voltage is applied, due to the valency of Si(IV) versus Al(III) [7]. The reversible voltage for electrodeposition is slightly lower for both Mn and Si than that for Al, which makes it feasible to co-deposit either metal with aluminum in the aluminum reduction cell [8]. Haarberg et al. [9] reported experiments where MnO, MnO_2, and Mn_2O_3 were added to the electrolyte in an industrial Hall-Héroult cell. The study found that manganese ended up in the metal regardless of the initial precursor introduced.

The reduction mechanisms of MnO and MnO_2 in fluoride-based melt at a molten aluminum cathode have been reported to be the following [9].

$$Mn^{2+} + 2e^- = Mn \tag{2}$$

$$Mn^{4+} + 4e^- = Mn \tag{3}$$

If Mn_2O_3 is used as a manganese precursor, then the reduction reaction would proceed according to the following:

$$Mn^{3+} + 3e^- = Mn \tag{4}$$

The reduction mechanism for silica reduction in an alkali halide mixture has been reported to be in two steps [10]:

$$Si^{4+} + 2e^- = Si^{2+} \tag{5}$$

$$Si^{2+} + 2e^- = Si \tag{6}$$

Current efficiency (CE) is one of the most important metrics for the performance of an electrolysis process and is a representation of how efficiently the supplied electricity has been used to deposit the cathodic product. For aluminum, it is the actual weight of produced aluminum divided by the aluminum that would theoretically be produced based on Faraday's law. Then CE% may be written as

$$CE\% = \frac{W_{\text{actual}}}{W_{\text{theoretical}}} \times 100 = \frac{W_{\text{actual}}}{MIt/nF} \times 100 \tag{7}$$

where W_{actual} is the actual mass of metal produced whereas $W_{theoretical}$ is the theoretical mass of metal produced according to Faraday's law. M is the molar mass of aluminum, I is the applied current in A, n is the valency of the aluminum species, and F is the Faraday constant 96,487 C/mol.

In practice, the theoretical amount of aluminum determined by Faraday's law can never be achieved, as there will always be losses. Some aluminum metal dissolves from the cathode into the electrolyte and diffuses through the cathode boundary layer where it gets re-oxidized by dissolved CO_2. CO is released and alumina is produced. This is the so-called back reaction which is the main contribution to current efficiency reduction:

$$2Al(diss.) + 3CO_2(g\ or\ diss.) = Al_2O_3(diss.) + 3CO(g) \tag{8}$$

Dissolved impurity species more noble than aluminum will also be reduced at the cathode [8]. Although the current used to deposit the impurity is generally seen as representing a loss in current efficiency, that is not the case if the intention is to co-deposit an alloying element along with aluminum and produce an alloy.

The average current efficiency for such an alloy can be calculated according to

$$CE_{\text{alloy}}\% = \frac{W_{\text{alloy}}}{W_{\text{alloy·theroretical}}} \times 100 \tag{9}$$

where W_{alloy} is the total mass of metal produced experimentally whereas $W_{\text{alloy}\cdot\text{theoretical}}$ is the theoretical mass of the alloy produced. The theoretical mass of the produced alloy is given by Faraday's law as

$$W_{\text{alloy·theoretical}} = \frac{M_{\text{alloy}}It}{z_{\text{alloy}}F} \tag{10}$$

where M_{alloy} is the average molecular mass of the alloy and z_{alloy} is the average charge transferred for the deposition of the alloy. The two quantities may be estimated for the Al–Mn/Si alloy, according to the so-called electrochemical equivalent given by

$$W_{\text{equiv.}} = \frac{\left[\frac{M_{Al}}{z_{Al}}\right] \cdot \left[\frac{M_{Mn/Si}}{z_{Mn/Si}}\right]}{\left(x_{Al}\frac{M_{Mn/Si}}{z_{Mn/Si}}\right) + \left(x_{Mn/Si}\frac{M_{Al}}{z_{Al}}\right)} \tag{11}$$

Thus CE % for the alloy can be given by

$$CE\ \%_{\text{alloy}} = \frac{W_{\text{alloy}}}{W_{\text{equiv.}}\frac{It}{F}} \times 100 \tag{12}$$

where M_{Al}, $M_{\text{Mn/Si}}$, z_{Al}, $z_{\text{Mn/Si}}$, x_{Al}, and $x_{\text{Mn/Si}}$ are the molar masses of Al and Mn/Si, their charges, and their mass fractions, respectively.

This work is a study on the direct electrochemical deposition of aluminum–manganese and aluminum–silicon alloys in fluoride-based melts in a laboratory cell designed for current efficiency measurements, using industrial standards for electrolyte composition and current density. Parts

of the findings reported here have been published elsewhere [11, 12]. The effect of the presence of Mn and Si on the current efficiency with respect to Al, the current efficiency for the alloy, and the shape of the surface of the solidified deposit are reported.

Experimental

Experiments were carried out in a laboratory cell originally designed by Solli et al. [13] for current efficiency measurements for aluminum deposition. The laboratory cell is schematically illustrated in Fig. 1. The cell is contained in a graphite crucible lined with sintered alumina, and a wetted steel cathode plate at the bottom. Dipped into the electrolyte from above is a cylindrical anode with a central vertical hole as well as horizontal holes penetrating the anode for efficient anode gas transport and convection in the cell.

As the aluminum is electrodeposited, it wets the cathodic steel plate forming an approximately flat deposit, presumably with even current distribution. A steel pin is placed in a hole connecting the steel plate and the graphite crucible, penetrating a layer of insulating alumina cement. The cement layer should prevent loss of the deposit and reduce the risk of aluminum carbide (Al_4C_3) formation. The composition of the electrolyte inserted in the cell at the start of the experiment is given in Table 1. The electrolyte components were dried at 200 °C for 24 h before being transferred to the crucible. The cell was then placed inside a sealed gas tight vertical furnace. The furnace was continuously flushed with argon gas.

As the cell reached the process temperature, the anode, suspended from a steel current collector penetrating the top lid, was lowered to the bath. The temperature was recorded during electrolysis using a thermocouple made of Pt/Pt10Rh placed inside a lateral slot of the crucible.

The operating temperature ranged from 965 to 980 °C with a fixed electrolysis duration of 4 h. The superheat varied correspondingly from 13.0 to 28.0 °C, as estimated from an empirical relation in [14]. The cathodic current density (CCD) was kept at 0.9 A/cm^2 and a cryolite ratio (CR) of 2.2 was used for all runs. The standard electrolyte was 12.0 wt.% AlF_3, 5.0 wt.% CaF_2, 4.0 wt.% Al_2O_3, and balance of NaF–AlF_3-based cryolite.

For the aluminum–manganese experiments, Mn_2O_3 was initially mixed with the bath constituents prior to electrolysis. Three concentrations were considered based on Mn content which were 1 wt.% Mn, 2 wt.% Mn, and 3 wt.% Mn.

For the aluminum–silicon experiments, three concentrations of SiO_2 were considered: 1 wt. % Si, 3 wt.% Si, and 4 wt.% Si. An additional test was carried out at 980 °C at an initial content of Si of 1 wt.% but with an initial content of alumina of 2 wt.% unlike all other tests which were run with a standard alumina content of 4 wt.%.

The bath was sampled regularly at constant intervals using quartz sampling tubes. The collected metal deposits

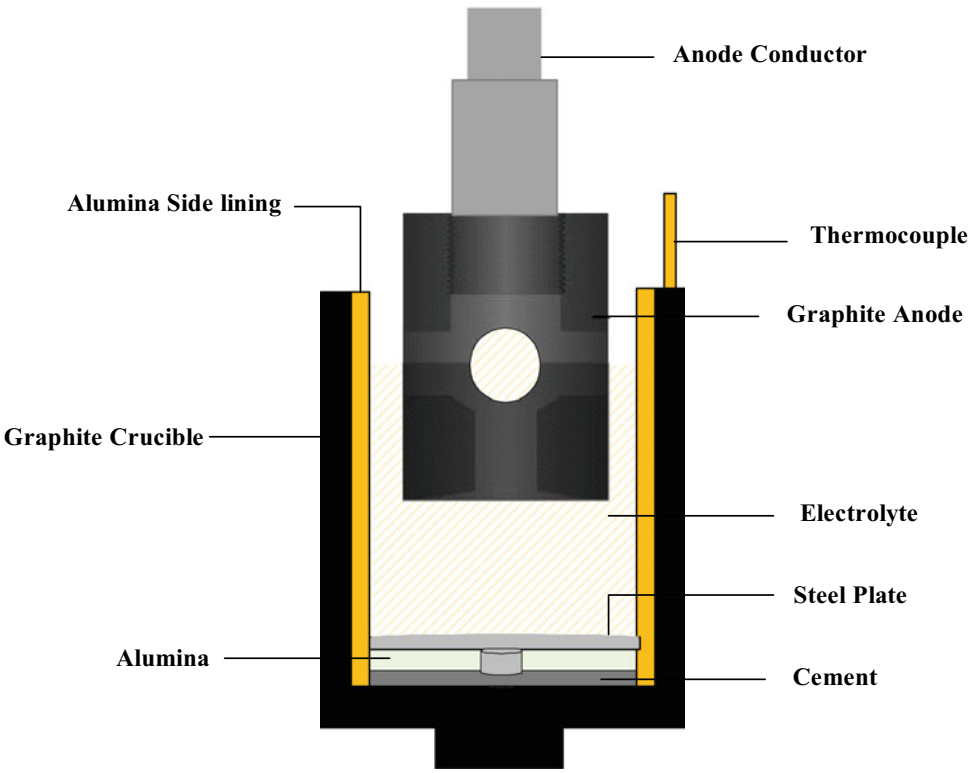

Fig. 1 The laboratory cell design for CE measurements

Table 1 Electrolyte components

Chemicals	Pre-treatment	Quality/supplier
AlF_3	Sublimed at 1090 °C for 24 h	Industrial grade, Alcoa–Norway
NaF	Dried at 200 °C for 24 h	99.5%, Merck–Germany
CaF_2	Dried at 200 °C for 24 h	Precipitated pure, Merck–Germany
Al_2O_3	Dried at 200 °C for 24 h	Anhydrous (γ-alumina), Merck–Germany
For Mn experiments Mn_2O_3	Dried at 200 °C for 24 h	325 Mesh powder, 98%, Alfa Aesar–Germany
For Si experiments SiO_2	Dried at 200 °C for 24 h	−325 Mesh powder, 99.5%, Alfa Aesar–Germany

were subjected to mechanical and chemical post-treatments. Bath samples were crushed into a fine powder and dissolved in a mixture of strong acids including HCl, HNO_3, and HF. The solutions were digested and agitated to ensure a complete dissolution. ICP-MS was conducted for samples afterwards to determine the Mn or Si content in the bath.

Results and Discussion

Cell Performance

Blank Tests

Three blank experiments were carried out without additives at 965, 970, 975, and 980 °C. The obtained current efficiencies along with the mean at each temperature value and a trendline are shown in Fig. 2.

The trendline found by least square regression yielded a reduction increase in the current efficiency of 0.2% for every 1 °C reduction in the operating temperature, which is in good agreement with literature [15]. These results, without the additives, serve as benchmarks to check for the effect of the addition of impurities on the current efficiency.

Mn and Si Addition

Bath Analysis

Mn experiments were run for 1wt.% Mn addition to the bath, at 965 and 980 °C. Bath samples were analyzed for Mn content using ICP-MS. As seen in Fig. 3, around 80% of the initial Mn content was depleted during the first half of the experiment (120 min) at 965 °C whereas 50% remained at 980 °C.

A similar analysis was done for Si for the experiment carried out at 980 °C and 4 wt.% Si. The change in the concentration of Si with time in the bath is also shown in Fig. 3. The concentration of Si in the bath does not show a decay trend as for Mn, or for Ti as reported in a separate paper [16] except towards the end, when the content of Si in

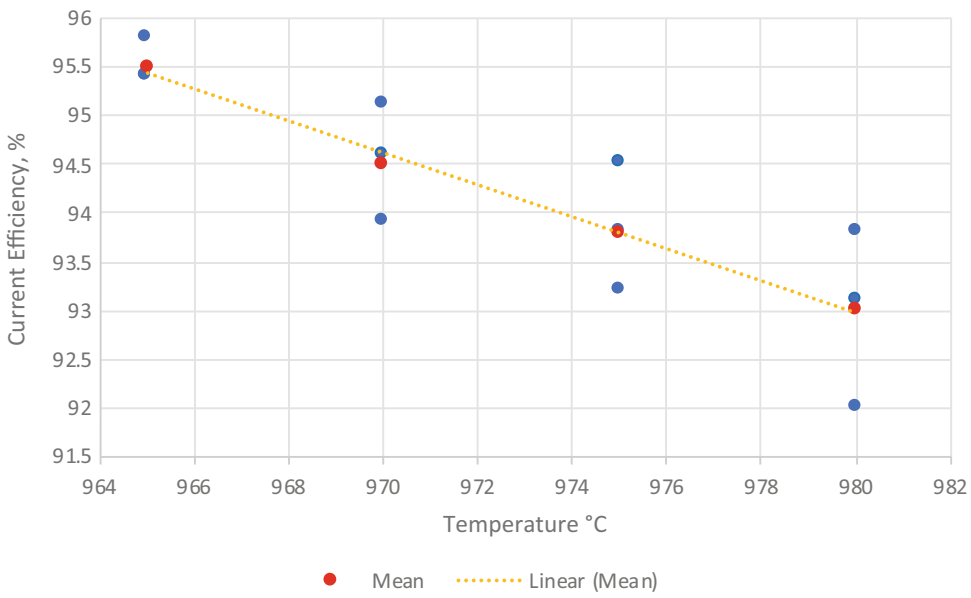

Fig. 2 CE obtained in blank tests without additives of Si and Mn as a function of temperature. The mean for each temperature along with a trendline is also plotted

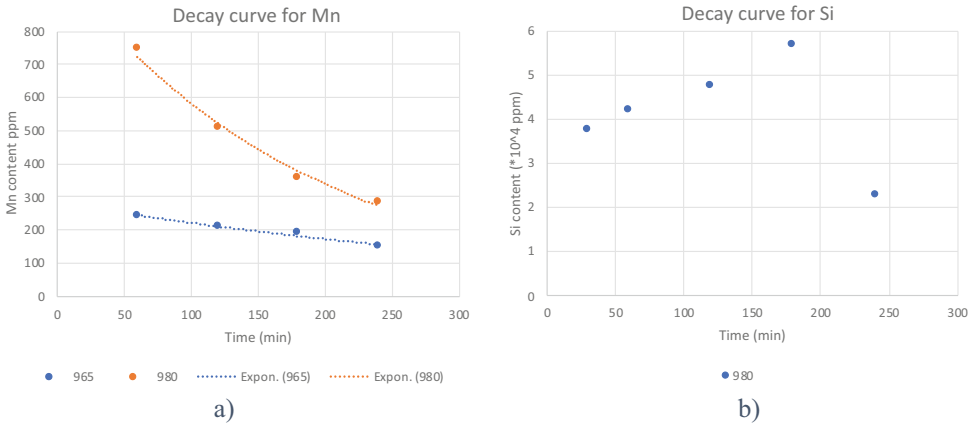

Fig. 3 Decay of Mn in the bath at 1 wt.% content at 965 and 980 °C in **a**, and concentration of Si in the bath at initial added content of 4 wt.% Si content at 980 °C in **b**. Note that the units on the vertical axis are different for Si than for Mn

the bath dropped down to 2.3 wt.%. This is likely caused by the silica not being completely dissolved in the electrolyte, or slow dissolution. The solubility of silica at the CR and in the temperature range for these experiments is not available in the literature, but at 1010 °C it is <5 wt.% [17], which corresponds to 2.3 wt% Si. The silica solubility at lower temperatures is likely lower than at 1010 °C, so the electrolyte was likely supersaturated during the experiment.

Deposit Analysis

ICP-MS analysis was carried out for the solidified Al–Mn deposits. Table 2 shows the content of Mn in the metal at different temperatures and different initial Mn contents added to the bath. The results show that an increase in the content of Mn in the metal was observed upon increasing initial concentration regardless of the operating temperature. At 1.0 and 2.0 wt.% Mn initially added to the bath, respectively, the final contents of Mn in the metal were ≈8.0 and ≈13.0 wt.%, respectively, regardless of the operating temperature which may imply less effect of temperature on the solubility of Mn in the bath. These analyses enabled an estimate of current efficiency for alloy deposition for the Al–Mn alloys. The apparent CE is based on the mass of the deposit, assuming that it is aluminum. As the molar mass of Mn is higher than for Al, this leads to estimates higher than 100%, which should not be confused with the actual alloy current efficiency.

Current Efficiency of Al–Mn Alloys

The current efficiencies of Al–Mn alloy deposition were estimated using Eqs. (9)–(12) and are given in Table 2 and Fig. 4. The average current efficiency for the alloy is a representation of the current efficiency of each element based on its content in the alloy using Eq. (10). In general, the

Table 2 Co-deposition of Mn

Run #	Temp. (°C)	Initial Mn content added to the bath (wt.%)	Apparent CE % for electrolysis	Conversion % of Mn at actual co-deposition	Deposit Mn content (wt.%)	Average CE% of Al–Mn	CE % for Al
1	965	1.0	96.8	81.6	8.0	92.9	89.1
2		2.0	98.4	69.1	13.3	91.8	85.4
3		3.0	107.0	56.7	15.0	98.8	91.0
4	970	1.0	96.2	78.7	7.7	92.4	88.8
5		2.0	99.9	69.6	13.2	93.2	86.8
6		3.0	101.3	60.5	16.9	92.6	84.2
7	975	1.0	92.7	75.9	7.7	89.1	85.5
8		2.0	99.4	70.1	13.3	92.7	86.2
9		3.0	104.5	64.3	17.4	95.3	86.3
10	980	1.0	91.3	72.9	7.5	87.8	84.4
11		2.0	100.2	70.5	13.3	93.4	86.9
12		3.0	93.7	68.1	20.6	83.8	74.4

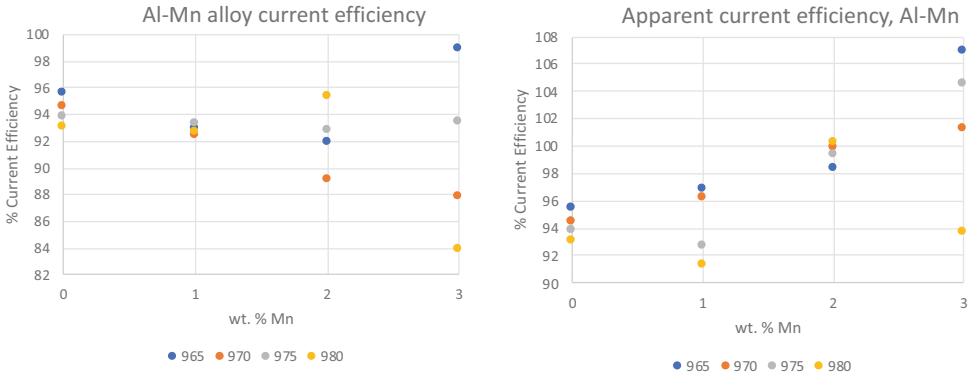

Fig. 4 Al–Mn alloy current efficiency on the left and apparent current efficiency on the right for 0–3 wt.% initial Mn concentration in the electrolyte at 965–980 °C

alloy deposition efficiency was slightly lower compared to the blank experiments, but nevertheless on average for each Mn concentration category in a similar range. However, the scatter in the alloy current efficiencies with temperature increased with Mn content in the bath. As seen in Table 2, co-deposited manganese content was in the range of 8–21 wt. %. The ratio of manganese found in the metal to manganese initially added to the bath in the form of Mn_2O_3 is referred to as the conversion ratio. The results indicate that 82% of the initial 1.0 wt.% Mn addition to the bath at 965 °C has ended up in the metal. It can also be seen that for the 1.0 wt.% Mn experiments, the conversion efficiency was reduced by approximately 1% for every 5 °C increase in the operating temperature. This trend was not observed for Mn conversion at 2.0 and 3.0 wt.% Mn experiments, the conversion efficiency improved for higher temperatures by almost 4% for each 5 °C increase in the operating temperature. This could be explained by faster oxide dissolution at higher temperature.

For comparison with the Al–Si experiments, apparent current efficiencies were estimated and are also listed in Table 3. Apparent current efficiency is here defined as the ratio percentage of the total weight of the solidified deposit divided by the theoretical mass calculated based on reduction of aluminum according to Faraday's law, calculated by Eq. (5).

Mn has a molar mass of 55 g/mol while the molar mass of aluminum is 27 g/mol, and the valencies of both Mn and Al were +3. This gives an apparent current efficiency that exceeds 100%.

Effect of Si Content on the Apparent CE

The Al–Si samples were not analyzed for Si content using ICP-MS, so the current efficiencies for Al–Si deposition could not be estimated, and only the apparent current efficiencies are available. As depicted in Fig. 5, the apparent current efficiencies decrease upon an increase in the initial wt.% of Si added to the bath at 965, 970, and 980 °C. At 965 °C, a drop of 13% in the apparent current efficiency, with respect to the blank test run at the same temperature, was recorded upon the introduction of 1 wt.% Si in the bath. It was ≈10% at 970 °C and 4% at 980 °C for the same Si concentration. It should be noted that the expectation is for the apparent current efficiency to be reduced with increasing initial wt.% Si in the electrolyte, as the molar mass of Si is almost the same as that for Al, or M_{Si} = 28 g/mol and M_{Al} = 27 g/mol, while the valency of Si is +4, as compared to +3 for Al. Therefore, it takes 4/3 more electrons to deposit a mole of Si than a mole of Al. Due to this, a certain lowering of the apparent %CE would be expected. However, to explain a 10% drop in %CE from this mechanism, the Si content in the deposit would have to be 30 wt%, so there are other contributing factors as well. One test was run at 980 °C for 1 wt.% Si in the bath and 2 wt.% alumina, rather than 4 wt.% alumina as in all the other experiments, as it has been reported that alumina enhances the solubility of silica [17], so a lower alumina content will decrease silica dissolution in the electrolyte. It was found that this decreased the apparent %CE from 87.9 to 76.5%, which supports the hypothesis that this less than desirable apparent %CE is related to undissolved oxides in the electrolyte and associated sludging.

Table 3 CE of Al at different initial contents of Si in Fig. 5

Temperature (°C)	Si initially added (wt.%)	Apparent CE %
965	0	95.5
	1	82.2
	4	59.2
970	0	94.5
	1	84.2
980	0	93.0
	1	87.9
	3	62.2
	4	61.3
	1 (2wt.% Al_2O_3)	76.5

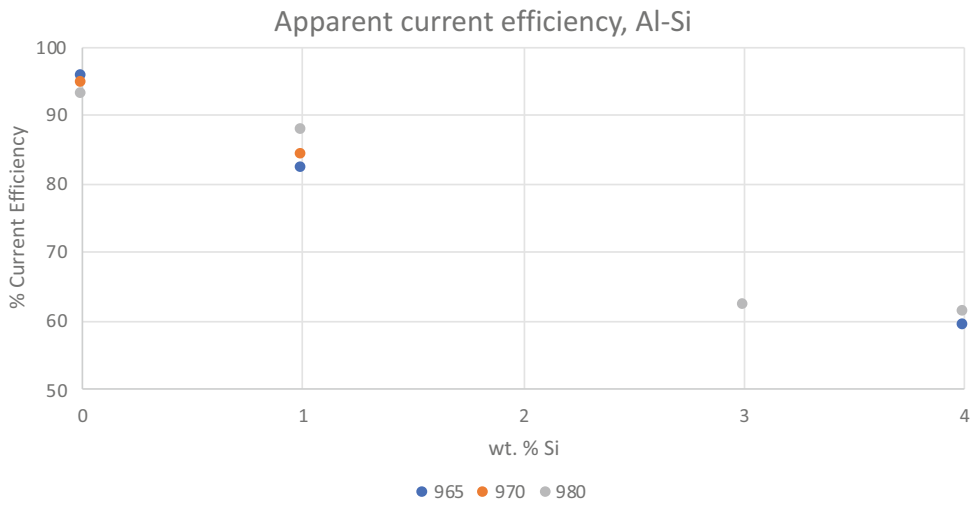

Fig. 5 Apparent current efficiency of Al at different temperatures and Si initial contents added to the bath

Fig. 6 Deposits obtained at T = 965 °C for a blank test to the left, 3 wt.% Mn initially in the bath in the center, and 1 wt.% Si to the right

Solidified Deposit Shape and Cell Voltage Behavior

The solidified deposits surfaces of all blank tests formed a flat even deposit. The deposits formed during Al–Mn deposition were flat at lower initial wt.% Mn content but showed a tendency to be more irregular with higher initial wt.% Mn in the electrolyte, while even the smallest tested addition of 1 wt.% Si caused the deposit to form a ball separate from but on top of the aluminum wetted steel cathode plate. Photographs of a blank deposit obtained at 965 °C, along with deposits obtained at the same temperature for 3 wt.% Mn and 1 wt.% Si in the electrolyte can be seen in Fig. 6. In Fig. 7, the cell voltage behavior for blank experiments, for Al–Mn deposition and Al–Si deposition, is compared. The cell voltage behavior for deposits suggests a suppression in the conductivity of the electrolyte due to the presence of dissolved silicon containing species. The higher the temperature the larger the decrease in the conductivity seemed to be as indicated by higher cell voltage.

Solidified Al–Si Deposit Surface Characterization

A sample obtained at T = 965 °C with 4 wt.% Si initially in the electrolyte was characterized by SEM/EDX. Two areas on the solidified deposit (P1 and P2) were analyzed, a SEM image along with Al and Si mappings are shown in Fig. 8. At P1 SEM showed silicon present along with some alumina and/or silica frozen on the surface reflected by the presence of oxygen as seen in Fig. 8 The EDX of this area gave approximately 10 wt.% Si and 90 wt.% Al. Area 2 The EDX mapping spectrum of P2 showed about 13.4 wt.% Si and 86.6 wt.% Al. The SEM and EDX mapping from this area showed a structure of parallel plates of a Si-containing phase, resembling a eutectic structure, but the composition

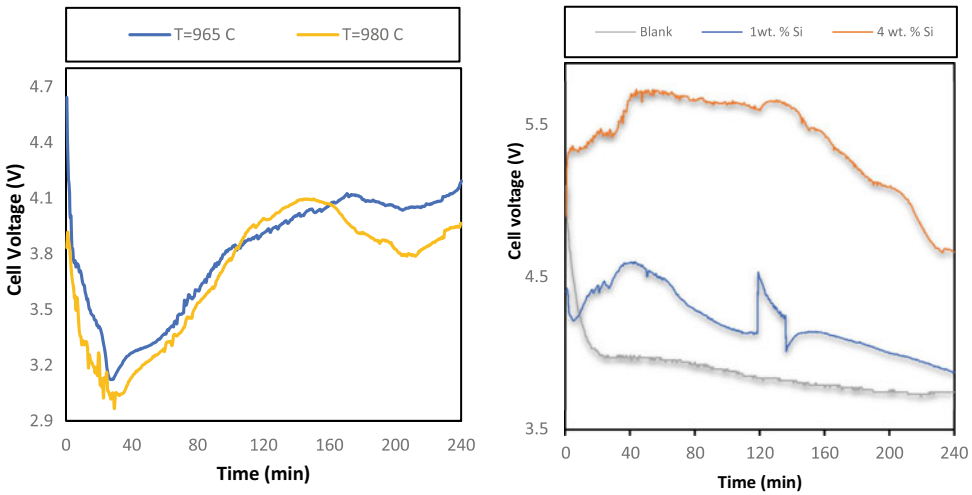

Fig. 7 Cell voltage behavior for initial 3 wt.% Mn content in the electrolyte at 965 °C and 980 °C on the left, and 1 wt.% Si (orange), 4 wt.% Si (blue), and blank test (grey) on the right, all at 965 °C (Color figure online)

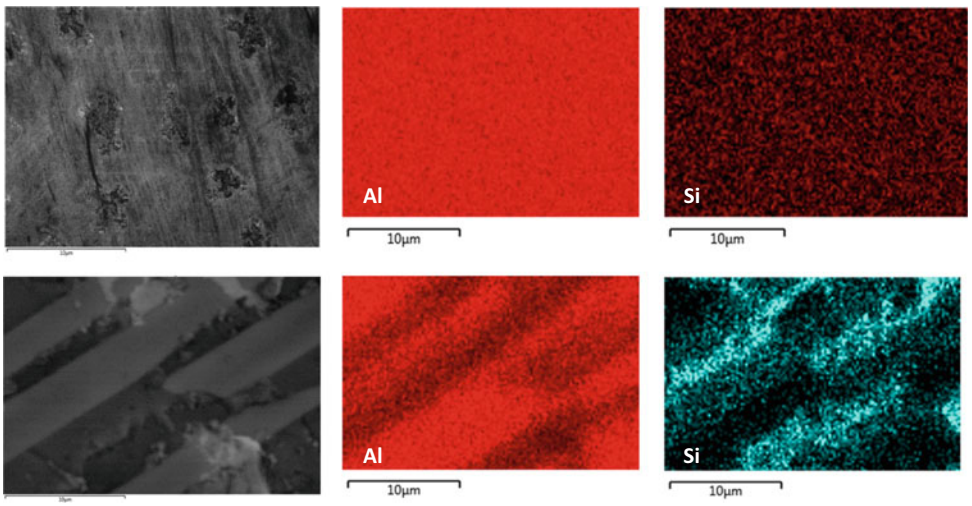

Fig. 8 EDX elemental mapping images of area 1 (P1) above and area 2 (P2) below

of this area is quite close to the 12.6 wt.% eutectic in the Al–Si binary phase diagram. Apparent %CE for this experiment was very low, at 56%, so for a Silicon content of 11–12 wt% Si in the deposit, the alloy current efficiency is still very low.

Conclusion

This paper describes laboratory experiments as a first step towards studying the feasibility of producing Al–Mn and Al–Si alloys directly by feeding Mn_2O_3 and SiO_2 into the Hall-Héroult aluminum reduction cell along with alumina and co-depositing the Mn or Si along with aluminum to form an alloy.

Analysis of the Al–Mn deposits shows an increase in the content of Mn in the metal upon increasing the initial concentration of added manganese oxide to the bath regardless of the operating temperature. At contents of 1.0 and 2.0 wt. % Mn initially added to the bath, the final contents of Mn in the metal were approximately 8 wt.% and 13 wt.%, respectively, regardless of the operating temperature which imply less effect of the latter on the solubility of Mn_2O_3 in the bath. At 3.0 wt% Si in the bath, however, the Si content in the deposit increased with temperature, indicating that the temperature effect on the solubility plays a role in higher concentration suggesting a temperature effect on the solubility of Si in the bath.

The average current efficiencies of Al–Mn alloys have comparable current efficiencies to the baseline blank efficiencies for aluminum deposition without additives, if slightly below, which implies that this path could be feasible to produce such alloys. At relatively low initial concentrations of Mn added to the bath at 965 °C around 80% ended up in the metal during the 4 h experiment. It can also be seen that at 1.0 wt.% Mn initially added, a reduction of about 1.0% in the conversion was estimated for every 5 °C

increase in the operating temperature. The enhancement in the conversion of Mn was insignificant at 2.0 wt.% Mn, and a 4% increase was observed in the conversion efficiency for every 5 °C increase in process temperature at 3.0 wt.% Mn content in the bath at the start of the experiment.

Adding silica to the electrolyte so that the initial Si content in the electrolyte was 1 wt% or more clearly had a detrimental effect on the apparent current efficiency of the process, and even though the current efficiency for the deposition of the Al–Si alloy was not estimated, as the metal deposits were not analysed for Si content, it was clearly unsatisfactory.

Adding silica to the electrolyte negatively affects the apparent current efficiency for aluminum regardless of the operating temperature which can be due to the co-deposition of silicon and incomplete dissolution of silica in the electrolyte which causes sludge. The results suggest that for every 1 wt.% Si initially added to the electrolyte, the average reduction in the apparent current efficiency is in the range of 9%. Results also suggest that the higher the initial content of silica added to the bath, the lower the apparent current efficiency turns out to be. A lower apparent current efficiency was recorded at lower initial alumina concentration while keeping the initial added silica content fixed at the same operating conditions. This can be explained by higher alumina content increasing silica solubility, which reduces sludging. SEM/EDS results of a deposit sample suggested the formation of Si hypoeutectic alloy.

Acknowledgements The financial support from the Norwegian University of Science and Technology (NTNU) is greatly acknowledged, as is the Icelandic Technology Development Fund.

References

1. K. Grjotheim and Halvor. Kvande, *Introduction to aluminium electrolysis: Understanding the Hall-Herloult process*. Dusseldorf: Aluminium-Verlag, 1993.
2. J. R. Davis, *Alloying: Understanding the Basics*. ASM International, 2001. [Online]. Available: https://books.google.is/books?id=Sg9fAVdf8WoC.
3. James D. Kline, William C. T. Yeh, and Ulysses A. Preston, "Method of adding manganese to aluminum," 3,865,583, Feb. 19, 1974.
4. William R. King, "Aluminium-Manganese Alloy," 3951764, Apr. 20, 1976.
5. J. G. Kaufman, E. L. Rooy, and A. F. Society, *Aluminum Alloy Castings: Properties, Processes, and Applications*. ASM International, 2004. [Online]. Available: https://books.google.is/books?id=JM0u1vwrS5UC.
6. D. R. Askeland, P. P. Fulay, and W. J. Wright, *The Science and Engineering of Materials*. Cengage Learning, 2010. [Online]. Available: https://books.google.is/books?id=wUYIAAAAQBAJ.
7. D. Elwell and G. M. Rao, "Electrolytic production of silicon," *J. Appl. Electrochem.*, vol. 18, no. 1, pp. 15–22, Jan. 1988, doi: https://doi.org/10.1007/BF01016199.
8. K. Grjotheim, and K. Matiasovsky, "Impurities in the aluminium electrolyte," *Aluminium*, vol. 59, no. 9, pp. 687–693, 1983.
9. G. M. Haarberg and P. Cui, "Mass Transfer Reactions Near the Cathode During Aluminium Electrolysis," in *Light Metals 2014*, J. Grandfield, Ed. Cham: Springer International Publishing, 2016, pp. 749–752. doi: https://doi.org/10.1007/978-3-319-48144-9_126.
10. R. Boen and J. Bouteillon, "The electrodeposition of silicon in fluoride melts," *J. Appl. Electrochem.*, vol. 13, no. 3, pp. 277–288, May 1983, doi: https://doi.org/10.1007/BF00941599.
11. O. Awayssa, G. M. Haarberg, R. Meirbekova, and G. Saevarsdottir, "Electrochemical production of Al–Mn alloys during the electrodeposition of aluminium in a laboratory cell," *Electrochem. Commun.*, vol. 125, p. 106985, Apr. 2021, doi: https://doi.org/10.1016/j.elecom.2021.106985.
12. O. Awayssa, G. Saevarsdottir, R. Meirbekova, and G. M. Haarberg, "Electrochemical Production of Al–Si Alloys in Cryolitic Melts in a Laboratory Cell," *J. Electrochem. Soc.*, vol. 168, no. 4, p. 046506, Apr. 2021, doi: https://doi.org/10.1149/1945-7111/abf40e.
13. P. A. Solli, T. Eggen, S. Rolseth, E. Skybakmoen, and Å. Sterten, "Design and performance of a laboratory cell for determination of current efficiency in the electrowinning of aluminium," *J. Appl. Electrochem.*, vol. 26, no. 10, pp. 1019–1025, Oct. 1996, doi: https://doi.org/10.1007/BF00242196.
14. A. Solheim, S. Rolseth, E. Skybakmoen, L. Støen, Å. Sterten, and T. Støre, "Liquidus temperatures for primary crystallization of cryolite in molten salt systems of interest for aluminum electrolysis," *Metall. Mater. Trans. B*, vol. 27, no. 5, p. 739, Oct. 1996, doi: https://doi.org/10.1007/BF02915602.
15. P. Fellner, G. M. Haarberg, J. Hives, H. Kvande, A. Sterten, and J. Thonstad, *Aluminium Electrolysis: Fundamentals of the Hall-Héroult Process*. Beuth Verlag GmbH, 2011. [Online]. Available: https://books.google.is/books?id=7MW1pwAACAAJ.
16. O. Awayssa, G. Saevarsdottir, R. Meirbekova, and G. M. Haarberg, "Electrodeposition of aluminium-titanium alloys from molten fluoride-oxide electrolytes," *Electrochem. Commun.*, vol. 123, p. 106919, Feb. 2021, doi: https://doi.org/10.1016/j.elecom.2021.106919.
17. Weill, D.F. and Fyfe, W.J, *J Electrochem Soc*, vol. III, no. 582, 1964.